NMR Analyses of-1,3-Bridged Calix[4]arene Conformations

R.P. Madigan,*,† B.B. Fulton,† W.E. Gerro,† P.F. Nino,† B. Vilaysane,† N. R. Dominguez,† A.J. Carlson,† B.J.P. Jones,‡ C.J. Lovely,† and F. W. Foss Jr†

†*Department of Chemistry and Biochemistry, University of Texas at Arlington*

‡*Department of Physics, University of Texas at Arlington, Arlington*

E-mail: ryan.madigan@mavs.uta.edu

Abstract

Calix[4]arenes are cyclic oligomers known for their unique molecular architecture that provides a versatile platform for various applications in supramolecular chemistry, host-guest interactions, and molecular recognition and detection when coupled to fluorescent molecules. The introduction of bridging groups at the 1,3 phenols within the calix[4]arene framework has the potential to yield distinctive structural features and enhanced functional properties. We used a multi-faceted approach, employing a combination of experimental and computational techniques to elucidate the three-dimensional structure and conformational dynamics of the 1,3-bridged calix[4]arene derivative. Nuclear magnetic resonance (NMR) spectroscopy, Density Functional Theory (DFT) based optimization, and Boltzmann-weighted NMR chemical shift calculations are used to determine the precise molecular structure of the binding domain in our novel calix[4]arene derivative, including conformation, bond distance, and angle details.

Introduction

Calixarenes are a class of macrocyclic molecules made up of phenols ortho-linked by individual methylene units.[1] These macrocycles are characterized in a "chalice" shape, enabling them to bind a multitude of metals, including both positively and negatively charged ions, and several transition metals.[2–4] This class of binding domain is attractive for its modularity, with a wide variety of functionalization possibilities for the upper (para-position) and lower (phenol-OH) rims, allowing tuning of solubility and binding affinity.[5,6] Substituting calixarenes physically changes their 3-dimensional structure and allows for tuning of the binding domain to accommodate different molecular targets. Of these molecules, derivatives of *p-tert*-butyl calix[4]arene, in which there are four repeated units of *p-tert*-butyl phenol connected by four methylene units, are the most common.[7] Structural investigation into rotational changes during substitution is needed to design and control synthetic routes to future binding domains.

Density functional theory (DFT) can be utilized to model these systems and attempt to computationally provide data on binding pocket characteristics. DFT is an iterative computational method for modelling quantum mechanics, for which many functional and basis sets have been developed and applied to a wide variety of use cases.[8–11] Experimental methods to determine the binding geometry of calix[4]arene derivatives are crucial to validating structures in solution. Calix[4]arene systems are notably complicated receptor design, as they may take on multiple conformations, especially during synthetic steps and purification. The most stable conformation, the cone (Figure 1), is stabilized by hydrogen bonding between lower rim hydroxyl groups. Other conformations occur when one or two phenols invert, causing a total of four conformations, the partial cone, 1,2-alternate, and the 1,3-alternate (Figure 1). Although adding a bulky group to the upper rim will increase barrier of rotation and decrease the other conformations presence somewhat, it is not a surefire way to prevent these other conformations. Modification of the lower rim also disrupts the stabilizing H-bonding and can impart charge-charge repulsion that enhance conformational rotations during synthesis.

Rapid and effective methods to identify conformationally restricted products are necessary for one preparing new calix[4]arenes.

Nuclear magnetic resonance (NMR) spectroscopy is useful for following changes in restricted conformer formations during synthesis. Conformers are distinguished by changes in proton and carbon chemical shifts. Both ^{1}H and ^{13}C NMR contain landmarks that distinguish conformations in the literature. For example, a large (∼2 ppm) shift in the ^{1}H NMR will occur on the hydroxyl group proton positioned on the lower rim of the macromolecule. This occurs as the degree of hydrogen bonding present reduces.[12] Carbon NMR reflects conformational changes, with the methylene protons being a unique marker. $ArCH_2Ar$ can be detected at approximately 31 ppm indicating two phenols syn to each other as seen in the cone conformer. Alternatively, this peak is shifted to approximately 37 ppm indicating two phenols anti to each other as in the 1,3-alternate. Finally, a combination of the two peaks indicate partial cone or 1,3-alternate.[13] There are caveats to these landmarks though. In ^{1}H NMR, deuterium exchange, as well as tetra functionalization of the lower rim, can remove these protons from the spectra. ^{13}C is more reliable, however, issues arise with these methods on resolution of instrumentation or presence of multiple carbons in that range due to large alkyl chain substitution. In our own data, we recently used a 500 MHz NMR to compare two separately isolated conformers from one reaction; there we received two ^{1}H NMR spectra that reasonably could both represent the cone conformer of a synthesized 1,3 bridged calix[4]arene derivative (Figure 2A). Experiment time and scan numbers were increased significantly before we were able to distinguish between the spectra (Figure 2B). With these limitations in mind, we examined several less conventional methods for structural determination of our 1,3-bridged calix[4]arene derivative. Although 1,2-bridges are common in the literature, there is a gap in the 1,3 bridged variety that can essentially result in three hypothesized conformers: cone, 1,3-alternate, and partial cone.

In addition to 1D NMR, we show how nuclear Overhauser effect spectroscopy (NOESY) demonstrates the interproton distance present in our molecule. We followed this with ro-

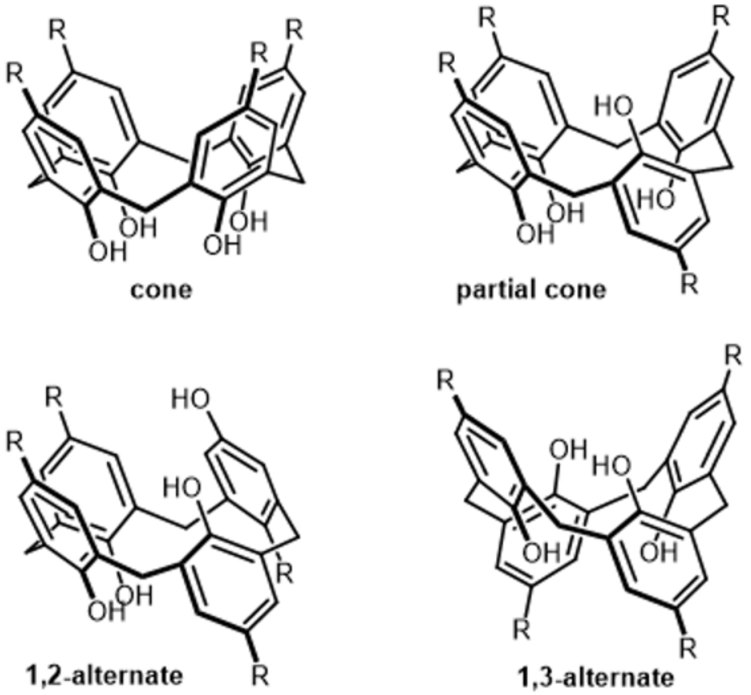

Figure 1: Conformations of *p*-*tert*-butylcalix[4]arene

tating Overhauser effect spectroscopy (ROESY) to attempt to easily quantitatively analyze these interproton distance and compare them to projected interproton distances calculated through DFT. Finally, we demonstrate the power of Boltzmann-weighted NMR chemical shift calculations that predict spectra for comparison to experimental ^{1}H and ^{13}C NMR data. With this data, we properly identify the cone conformer of a rare 1,3-bridged calix[4]arene and discuss the structural changes the bridging system seems to impart on the geometry of the cone.

Experimental

Reagents and Materials

All reagents and solvents were purchased from Sigma Aldrich, VWR, or Fisher Scientific. All reactions were carried out under a nitrogen atmosphere with anhydrous solvents in accordance to Scheme 1. ^{1}H NMR spectra were acquired on 500 MHz JEOL spectrometer

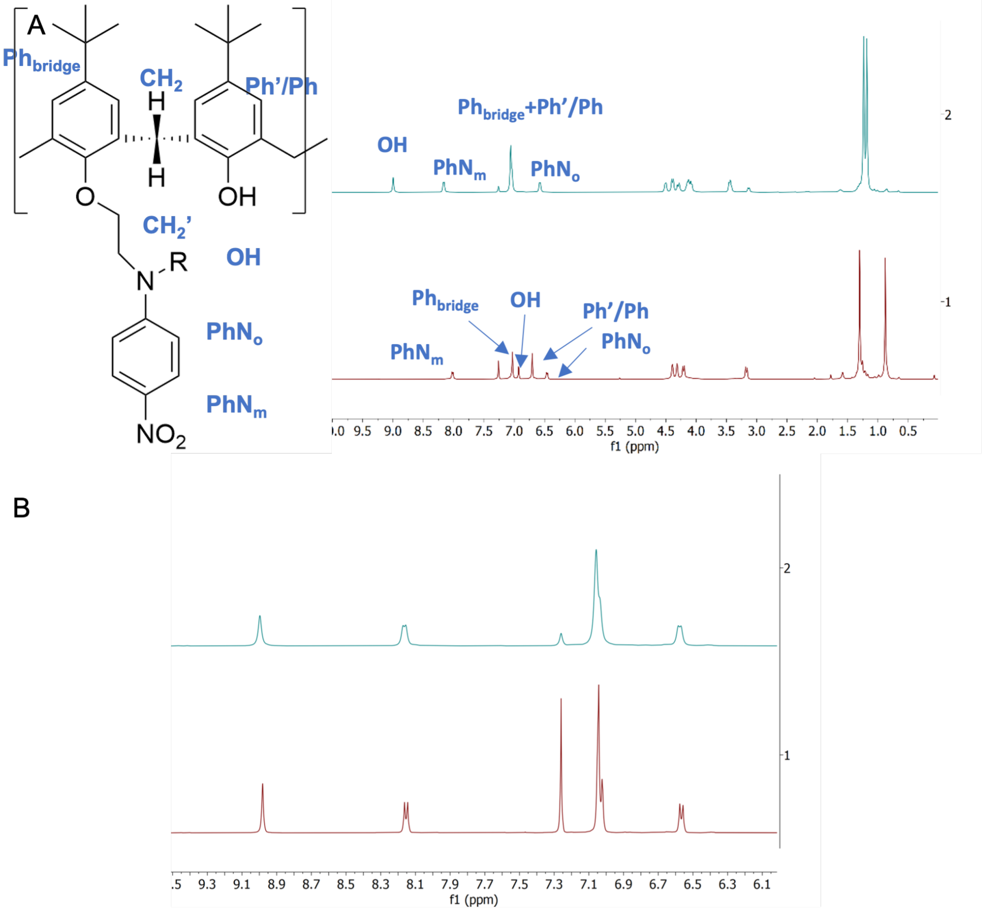

Figure 2: A) Spectra comparison between two conformational isomers of a 1,3 bridged calix[4]arene derivative. Peaks with similar integration leads to ambiguity of correct conformer. B) Spectra comparison of two ^{1}H NMR studies one the same isolated compound with 4 (top) and 32 (bottom) scans. Bottom spectrum begins to show two peaks in the 7.03 ppm region, which integrate approximately to 6 and 2 when compared to the same spot above that integrates to 8 lending evidence towards a partial cone byproduct.

and referenced to the internal solvent signals (7.26 ppm in CDCL$_3$). ^{13}C{1H} NMR spectra were acquired on a 125 MHz spectrometer referenced to the internal solvent signals with a central peak at 77.00 ppm in CDCL$_3$. NMR data are reported as follows: chemical shift (in ppm, δ), integration, multiplicity (s = singlet, d = doublet, t = triplet, q = quartet, m = multiplet, br = broad), coupling constant (in Hz, J). Confirmation of proton and carbon assignments for computational analysis was done by performing homonuclear correlation spectroscopy (COSY) and heteronuclear single quantum coherence (HSQC) NMR experiments. Examination of through space proton interaction was done using nuclear Overhauser

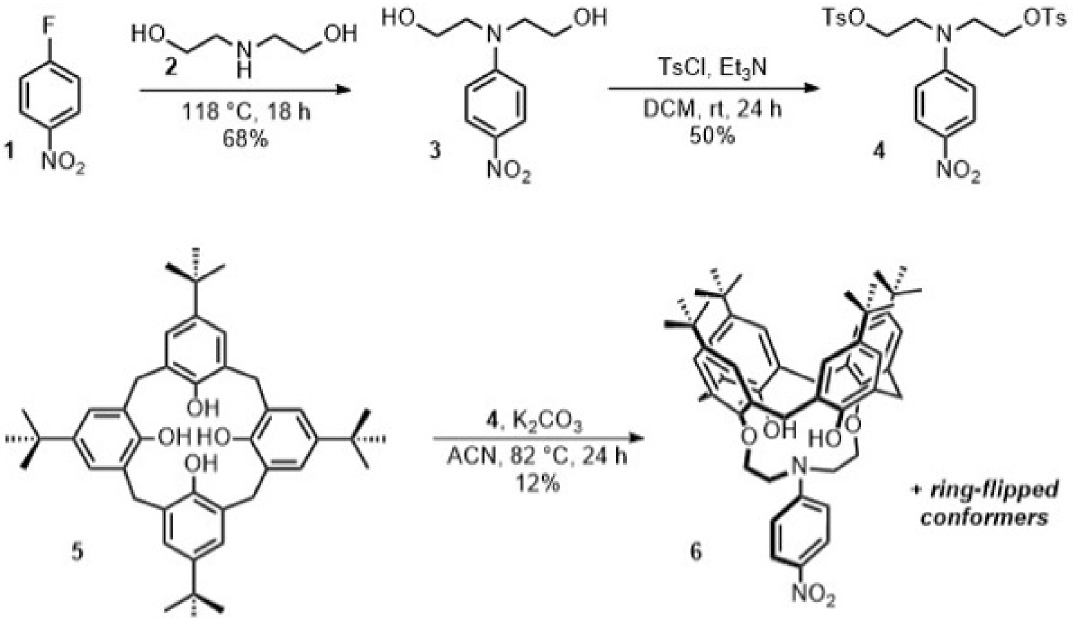

Scheme 1: Synthetic pathway for bridged calix[4]arene system

effect spectroscopy (NOESY) and rotating Overhauser effect spectroscopy (ROESY). Thin layer chromatography was performed on silica gel-coated aluminum plates (EMD Merck F254, 250μm thickness). Ultraviolet lights (254 nm) were used to visualize components. Flash column chromatography was performed over Silicycle SilicaflashP60 silica gel (normal phase, mesh 230-400). Preparatory TLC was performed on Silicycle glass backed TLC plates (60 A, 2000 μm thick, 20 cm x 20 cm). IR spectra were recorded in a Bruker Alpha-P FT-IR Spectrometer by attenuated total reflectance on a diamond sample plate. HRMS data were recorded by LCMS-IT-TOF in the Shimadzu Center for Advanced Analytical Chemistry at UT Arlington.

Synthesis

Synthesis of 2,2'-[(4-nitrophenyl) imino]diethanol (3)

Commercially bought 1-fluoro-4-nitrobenzene **(1)** (2.24 g, 0.016 mol) was stirred neat with 2,2'-iminodiethanol **(2)** (8 mL, 0.070 mol) and refluxed at 118°C for 18 h. Reaction was cooled to room temperature and poured into 360 mL of ice water and stirred for 30 minutes.

This was then filtered and the precipitate was dried completely before being recrystallized in ethanol-petroleum ether to receive 2.46 g (68%) of yellow crystals.[14] ^{1}H NMR (500 MHz, $CDCL_3$) δ; 8.11 (d, J=9.5 Hz, 4H), 6.67 (d, J=9.6 Hz, 4H), 5.30 (s, ^{1}H deuterium exchange), 3.95 (t, J= 5.0 Hz, 8H), 3.73 (t, J=5.0 Hz, 8H) ^{13}C{1H} NMR (125 MHz, $CDCL_3$) δ; 126.55, 111.51, 60.73, 55.44 IR (neat, cm-1):3242.40, 1582.26, 1478.72, 1166.17 HRMS (ESI) calcd for C10H15N2O4 $[M+H]^+$; predicted: 227.1031, found: 227.1027

Synthesis of 2,2'-[(4-nitrophenyl) imino]ditosylate (4)

Synthesized **3** (4 g, 0.018 mol) from above was dissolved in 50 mL of DCM. In order, TsCl (10.1 g, 53.1mmol) and Et_3N (5.4 g, 53.1 mmol) where added and the mixture was allowed to stir for 24 h. A further 150 mL of DCM was added to the solution, and solution was extracted three times with 250 mL DI water, once with 250 mL brine, and then dried over magnesium sulfate. Following filtration, the organic layer was evaporated and the resulting material was recrystallized in acetone-water to receive 4.8 g (50%) of yellow crystals.[15] ^{1}H NMR (500 MHz, $CDCL_3$) δ; 8.01 (d, J=9.5, 2H), 7.68 (d, J=8.3 Hz, 4H), 6.42 (d, J=9.5 Hz, 2H), 4.15 (s, 4H), 3.69 (s, 4H), 2.41 (s, 6H) ^{13}C{1H} NMR (125 MHz, $CDCL_3$) δ; 151.20, 145.81, 138.68, 132.65, 130.37, 128.22, 126.47, 111.06, 66.25, 50.70, 22.03 26.5 IR (neat, cm-1): 1708.86, 1508.69, 1395.03, 1205.72 HRMS (ESI) calcd for $C_{24}H_{27}N_2O_8S_2$ $[M+H]^+$; predicted: 535.1209, found: 535.1202

Synthesis of *p*-*tert*-butyl calix[4]arene (5)

p-*tert*-butylphenol (100 g, 0.666 mol), 37% formaldehyde solution (62 mL, 0.83 mol of HCHO), and sodium hydroxide (1.2, 0.03 mol) in 3 mL of water were stirred in an open-air flask for 15 min, before being heated to 120 °C for 2 h. The mixture was then cooled to room temperature and dissolved in 1000 mL of warm diphenyl ether. The mixture was stirred and heated back to 120 °C with a stream of nitrogen blowing over the mixture. Once solid formed, a condenser was added to the flask, and the heat was turned to 160 °C for 15 minutes, then finally put to reflux at 258 °C for 4 h. The crude material was again cooled to room temperature before 1.5 L of ethyl acetate was added. Following 30 min of stirring and 30 min of sitting, the mixture was filtered and washed twice with 100 mL of ethyl acetate, once with 200 mL of acetic acid, twice with 100 mL of water, and twice with 50 mL of acetone. This was then recrystallized in toluene to receive 65 g (52%) of white crystals.[16] The sample was complexed with toluene following the recrystallization, requiring long periods of low pressure and high temperature to remove toluene. ^{1}H NMR (500 MHz, $CDCL_3$) δ; 10.34 (s, 4H), 7.05 (s, 4H), 4.25 (d, J=13.7 Hz), 3,49 (d, J=13.3 Hz, 4H), 1.21 (s, 39H) $13C\{1H\}$ NMR (125 MHz, $CDCL_3$) δ; 147.06, 144.76, 128.08, 125.90, 34.40, 32.99, 31.79 IR (neat, cm-1): 3164.37 HRMS (ESI) calcd for $C_{44}H_{55}O_4$ [M-H]$^-$; predicted: 647.4100, found: 647.4144

Synthesis of 5,11,17,23-Tetra-tert-butyl-25, 27, (4-nitrophenyl) iminodiether ,26,28-dihydroxycalix[4]arene (6)

5 (648 mg, 0.001 mol) was added to 30 mL of distilled acetonitrile along with potassium carbonate (552 mg, 0.004 mol) and stirred at room temperature for 1 h. **4** (560.7 mg, 0.00105 mol) was added while stirring and the reaction was stirred for 48 hours. Following this, 10% HCl solution was added until pH 1 and then the reaction was evaporated to dryness. The mixture was then dissolved in 30 mL of chloroform and extracted three times with 30 mL of water, one time with 30 mL of brine, and then dried over magnesium sulfate. The organic layer was evaporated to dryness and run on a silica column (0-15% ethyl acetate to hexane). The cleaned up yet still crude material was then run on a prep TLC (15% ethyl acetate) and obtained as a yellow powder (11 mg, 12% yield). ^{1}H NMR (500 MHz, $CDCL_3$) δ; 8.02 (d, J=9.3 Hz, 2H), 7.03 (s, 4H), 6.93 (s, 2H), 6.70 (s, 4H), 6.46 (d, J= 9.3 Hz, 2H) 4.39 (s, 4H), 4.31 (s, 4H), 4.21 (d, J= 13.2 Hz, 4H), 3.17 (d, J=13.0 Hz, 4H), 1.30 (s, 18 H), 0.88 (s, 18H) $13C\{1H\}$ NMR (125 MHz, $CDCL_3$) δ; 151.33, 150.41, 149.70, 147.53, 142.09, 137.81, 132.14, 127.86, 126.44, 125.83, 125.30, 111.39, 73.78, 53.61, 34.02, 31.85, 31.02 IR (neat, cm-1): 2921.03, 1593.52, 752.22 HRMS (ESI) calcd for $C_{54}H_{67}O_6N_2$ $[M+H]^+$; predicted: 839.4999, found: 839.4972

NMR Experimentation

As above, all NMR spectra were acquired on 500 MHz JOEL spectrometer in $CDCl_3$. Confirmation of proton and carbon assignments for computational analysis was done by performing homonuclear correlation spectroscopy (COSY) and heteronuclear single quantum coherence (HSQC) NMR experiments. Interactions of protons in space were done using nuclear Overhauser effect spectroscopy (NOESY) and rotating Overhauser effect spectroscopy (ROESY). ^1H NMR were taken with 32 scans, spectral width 15 ppm (7507.5 Hz). $^{13}C\{1H\}$ NMR were taken with 2000 scans, spectral width 250 ppm (31446.5 Hz). ^1H COSY was taken with 1 scan, spectral width 11.5 ppm (5252.1 ppm). HSQC was taken with 4 scans, spectral width 11.5 ppm by 200 ppm (5252.1 ppm, 25150.9 ppm), F1 phasing: PH0 = 24.00°, PH1 = -7.50°; F2 phasing: PH0 = -30.00°, PH1 = -7.50°; Apodization along t1: sine bell 90.00° and sine square 90.00°; Apodization along t2: sine bell 90.00°; Polynomial fit baseline correction was applied to both F1 and F2. NOESY NMR taken with 4 scans, spectral width -9.5 ppm (5252.1 ppm), F1 phasing: PH0 = 272.23°, PH1 = -475.79°; F2 phasing: PH0 = 47.65°, PH1 = 8.06°; Apodization along t1: sine bell 90.00° and sine square 90.00°; Apodization along t2: sine bell 90.00°; Polynomial fit baseline correction was applied to both F1 and F2. ROESY was taken with 4 scans, spectral width 15 ppm (7507.5 ppm), F1 phasing: PH0 = 45.00°, PH1 = 7.50°; F2 phasing: PH0 = -12.75°, PH1 = 63.75°; Apodization along t1: sine bell 90.00° and sine square 90.00°; Apodization along t2: sine bell 90.00°; Polynomial fit baseline correction was applied to both F1 and F2.

Density Functional Theory Calculations

The molecular geometries of both **(5)** and **(6)** were optimized through the Gaussian 16 program (Revision C.01) with DFT (Density Functional Theory) using the Becke, 3-Parameter, Lee-Yang-Parr (B3LYP) hybrid functional, and the 6-31G basis set for H, C, N, and O. Subsequent frequency calculations were performed to confirm whether the calculated geometries represented a ground state (no imaginary frequencies) or a transition state (one imaginary frequency) to which the result was 0 imaginary frequency for both molecules. No solvent system was used for any of the calculations.

Predictive NMR Studies

The structures used for NMR chemical shift calculations were obtained by submitting calix[4]arene derivative 6 (input as the cone conformation) to the conformational search program CREST (Conformer Ensemble Sampling Tool) which generated a set of low energy conformers within a 6.0 kcal/mol range. From this set, the structures were manually inspected and separated into groups corresponding to isomers 1, 2, and 3. Geometry optimization (B3LYP/6-31G(d,p)), energy refinement (M06-2X/6-31G(d,p)) and NMR chemical shift calculations (mPW1PW91/6-311G(d)) were performed for each conformer of the three sets. The M06-2X/6-31G(d,p) energies were then used in conjunction with the Boltzmann equation to obtain weighted chemical shifts of each isomer. Analysis of the data was conducted on the scaled chemical shift values by comparing CMAE (Corrected Mean Average Error) and correlation coefficients (R^2) for each isomer. Combined proton and carbon values were obtained according to the following formulas: $MAE_{comb} = \sqrt{MAE_{^{13}C} \times MAE_{^{1}H}}$ and $R^2_{comb} = 1 - \sqrt{(1 - R^2_{^{13}C}) \times (1 - R^2_{^{1}H})}$. Additionally, DP4+ probability analysis was used to assign probabilities of correct assignment for each isomer.[17–22]

Results and Discussion

2-Dimensional Analysis

2D NOESY (500 MHz JEOL spectrometer) was performed on **(6)** and referenced to the internal solvent signals (7.26 ppm in $CDCL_3$) to analyze the through space interactions

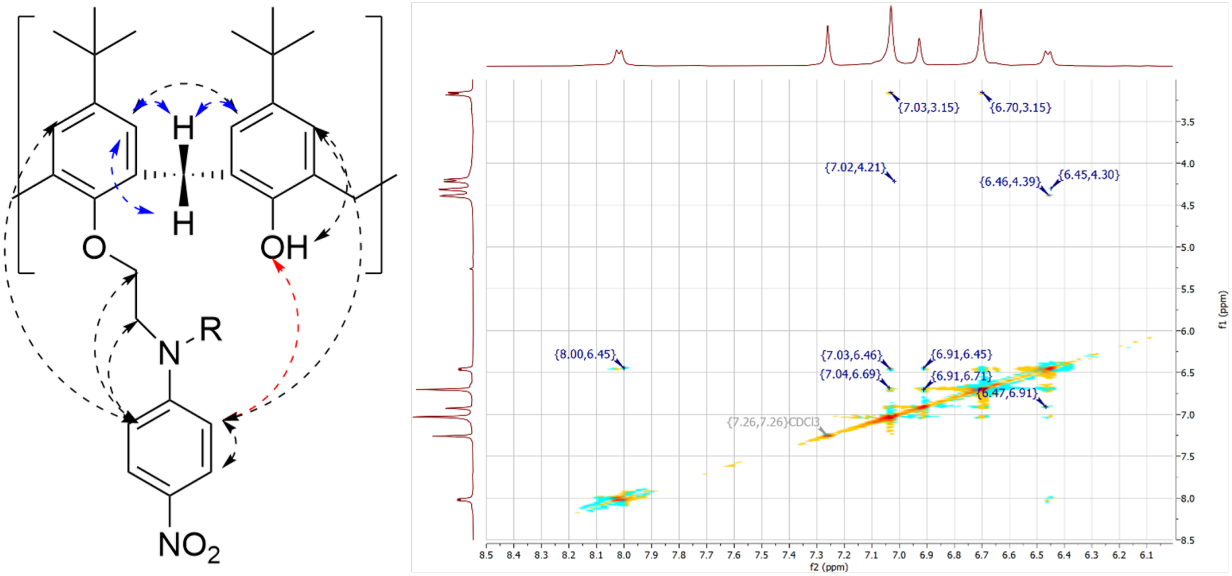

Figure 3: NOESY spectrum for molecule 6.

of the molecules as opposed to through bond interactions (Figure 3).[23] 2D NOESY is a technique that can measure magnetization exchange process between dipolar coupled spins and allows examination of proton interactions relative to each other in physical space, as opposed to bond proximity.[17] We hypothesized we would see interactions that suggest a specific conformation. The current pattern contained in the ^1H eliminated the partial cone, leaving the cone and 1,3-alternate as options. Our results showed interesting yet inconclusive interactions. An interaction between the hydroxyl proton and $PhN_\circ$ (6.47, 6.91, Figure 3 red dashed line) is notable, as the same interaction between $PhN_\circ$ and the *tert*-butyl groups is absent. This could suggest that the hydroxyl group is closer to the $PhN_\circ$ then the *tert*-butyl groups, giving tentative evidence towards the cone conformation. In addition, we see two interactions with the CH_2 proton and its neighboring aromatic protons, yet we do not observe one from the CH_2' and the same protons (Figure 3 blue dashed line).

To estimate the expected interproton distances in this molecule, we ran DFT on 6. As an internal standard, we also ran DFT on 5 as there is a known crystal structure available for comparison (Figure 4).[24] The DFT model of our molecule shows that the interaction of CH2' to Ph' that was missing from our NOESY spectrum, while these groups have an expected

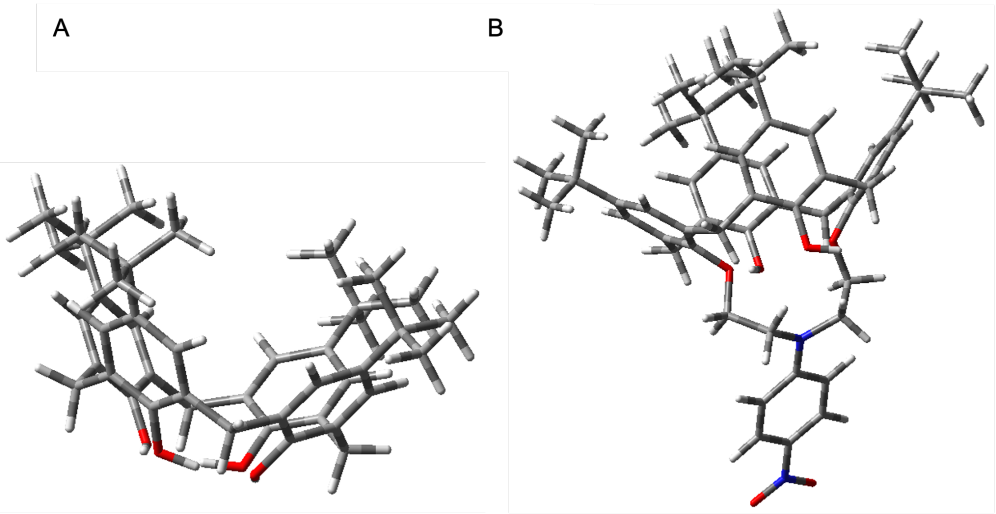

Figure 4: DFT model of **(5)** molecule (A) and **(6)** (B). B3LYP functional and 6-31G basis set .

spatial separation of approximately 3.72 Å . For a molecule of this size, a typical distance limit for detection is about 4 Å .[25] If we amplify all signals in our NOESY spectrum, we do begin to see a faint interaction between the CH_2' and Ph proton, but introduce a multitude of noise and artifacts to do so. Therefore, we believe our limit of detection to be below 4 Å , possibly due to low concentration of compound. We would expect to get a stronger signal between CH_2' and Ph in the case of a 1,3-alternate conformation, however we cannot use the information above to conclusively state conformation without a 1,3-alternate in hand. With that, we envisioned focusing on the CH_2 interaction in some form of quantifiable way. NOESY gave us tentative evidence in support of cone due the relative proximities of some key protons, however it is not fully conclusive because we do not have other conformers to compare experimental data with.

We then used a ROESY analysis for further interproton measurements, as literature suggested it to be superior for accurate study of spatial separations in molecules this size.[25] We utilized the peak amplitude normalization for improved cross-relaxation (PANIC) method to measure the distances between protons.[26] In brief, we examined the F1 slice (Figure 5) in which the methylene peak present at 3.18 ppm (Figure 5, green proton) was irradiated. We set the irradiated peak to an arbitrary intensity unit, in this case 1000 and then used the

Table 1: Computational and calculated distance between CH_2 methylene proton and neighboring protons. Computational was based on previously reported crystal structure and DFT analysis. Calculated was done using both the crystal structure and DFT as a standard methylene distance. Of note is the accuracy to the Ph proton when set to each standard.

Average CH_2 - X distance (Å)					
	Reference **(5)**		*Bridged Calixarene* **(6)**		
X	X-Ray	DFT	DFT	ROESY (X-ray)	ROESY (DFT)
CH_2’	1.60	1.75	1.76	1.60	1.76
Ph_{bridge}	2.39	2.38	2.31	2.22	2.44
Ph	2.39	2.38	2.61	2.39	2.63

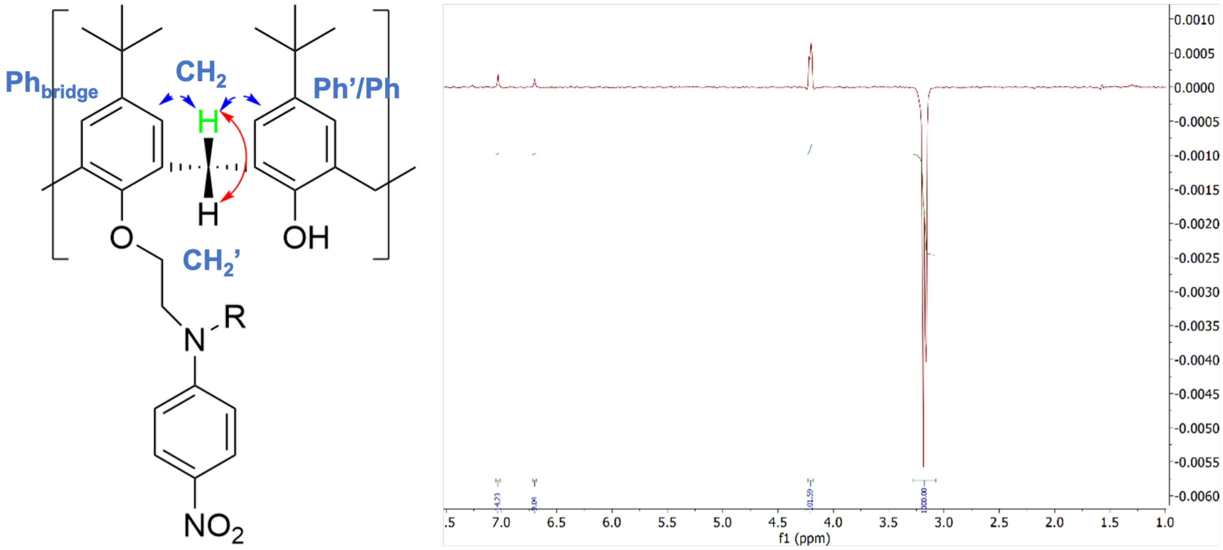

Figure 5: : 2D ROESY F1 slice at F2 chemical shifts (500 MHz, $CDCl_3$) of methylene proton at the 3.180 ppm signal, with integrals as the intensity of each proton in relation to standard at 3.180 ppm.

approximate formula $r_{NOE} = r_{ref} \times (\eta_{NOE}/\eta ref)^{1/6}$ in which r is interproton distance, and η is the NOE signal intensity. The reference distance in our experiments is provided by the average of the proton distances between CH_2 and the other methylene proton, represented by the red arrow in Figure 5. To fix the scale of this reference, two options are available: the structure we have simulated using DFT, and the crystal structure available in the literature. We applied both choices in order to quantify this particular source of systematic uncertainty (Table 1). We then measured the distance to both Ph_{bridge} and Ph (blue arrows) relative to this reference, using the above equation. We received 2.44 Å for CH_2 to the proton at Ph_{bridge},

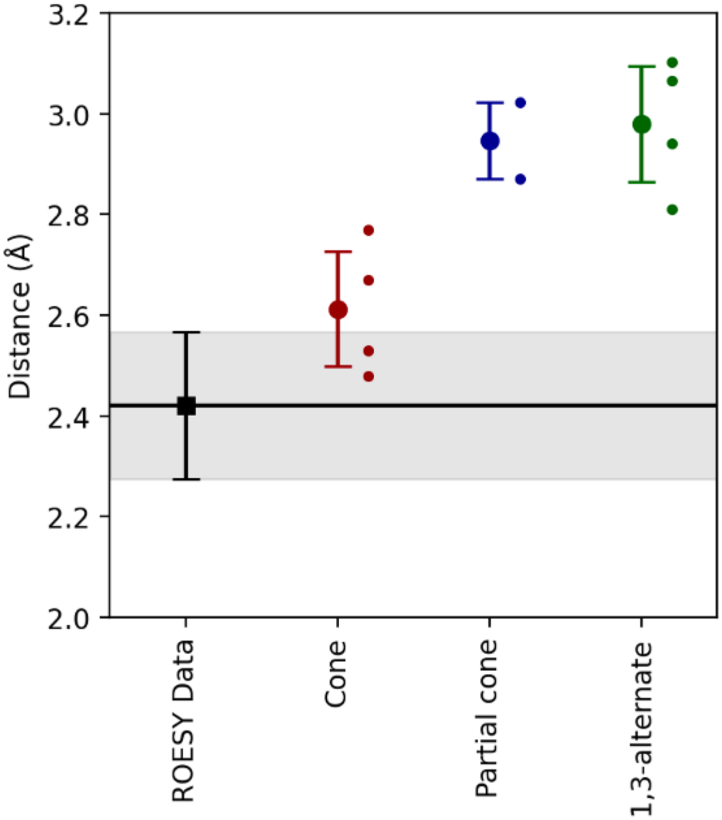

Figure 6: Average distance between CH_2 to the Ph proton in the 3 possible conformers. Here the ROESY measurement is shown, with error bar provided by the choice of reference distance, compared against the different proton distances predicted in optimized DFT computations of each conformer.

and 2.63 Å for the distance to Ph when utilizing our DFT model as reference, and 2.22 Å and 2.39 Å respectively when using the crystal structure data as reference. Both values of CH2 to Ph seem to be close to expected based on respective standards used, however the distance to Ph_{bridge} is more variable. This combined with DFT predicts our calix[4]arene motif has formed an oval shape instead of a perfect circle. We hypothesize that the bridge, pulling the 1,3 positions in a more ridged conformation, is the main reason we see this effect, as the movement more equatorial would minimize the distance between the stabilizing hydrogen bonding hydroxyl groups. A force not accounted for could be interacting with the phenol groups, changing their positioning that our DFT cannot consider, and is further present in **(5)**, providing some reasoning behind our calculations not matching the crystal structure.

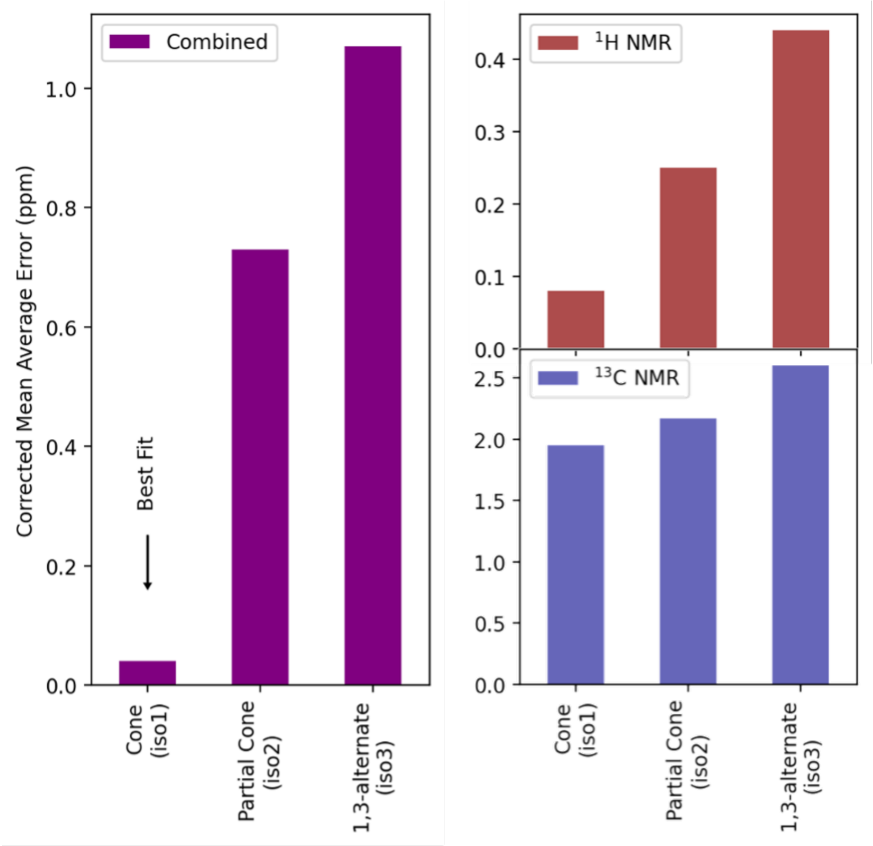

Figure 7: Plot of isomer preference by corrected mean average error (CMAE) value, showing that across both types of NMR studied and in the combined analysis, the cone is preferred.

As discussed, the interproton distances measured using ROESY appear to be consistent with those expected for the cone geometry, as expected from both DFT and crystal structure. An interesting question is whether this consistency provides sufficient evidence to reject the other possible conformers. We ran DFT calculations on the other conformers to provide us with distances to compare our calculations against (Figure 6). It appears regardless of reference used, the partial cone and 1,3-alternate lay outside of the measured ROESY value. We believe this allows our ROESY to provide conclusive evidence that we have received our cone conformer.

Predictive NMR studies

While neither NOESY or ROESY were conclusive in identifying a single conformer unambiguously, predictive ^{1}H and ^{13}C NMR chemical shift calculations were found to be effective for this purpose. The results of these analyses are summarized in terms of their corrected mean average error (CMAE) in Figure 7 with unanimous favor toward isomer 1. The supplemental information also provides corrected mean average error and various probabilistic metrics, with similar conclusions in all cases. In each method tested we see a preference towards cone, in both ^{1}H and ^{13}C spectra, and even stronger under a combined analysis. DP4+, a Bayesian probability method designed specifically for the task of distinguishing between candidate molecular structures by comparison of computed chemical shifts, shows between 99.9% and 100% confidence in the cone conformer. In connecting this data to the hallmarks known in the literature, we see that the methylene carbon connecting the four phenol aromatic rings in the bridged system can serve as a diagnostic chemical shift for distinguishing between the ring-flipped conformers. This is reflected in both our experimental observations where a ^{13}C chemical shift appears at 31.1 ppm and computationally where the cone conformation produces a value of 33.4 ppm, vs. the 37.5 (averaged value of the two CH_2 shifts) and 39.3 ppm values generated by the partial cone and 1,3-alternate conformations respectively. Also shown in Figure 8 are the corresponding energy values, calculated at the M06-2X/6-31G(d,p) level of theory for the lowest energy conformer of each isomer. The stability of these conformers is mirrored by previously reported values in literature for calix[4]arene systems with cone being the lowest.[27]

Conclusion

We have explored the use of several methods NMR spectroscopy to understand the conformational structure and geometry of 1,3-bridged calix[4]arene derivatives. Through comparison of ^{1}H and ^{13}C NMR computational spectra with data, we were able to conclusively establish that our molecule was in the cone conformation through probabilistic analysis of the

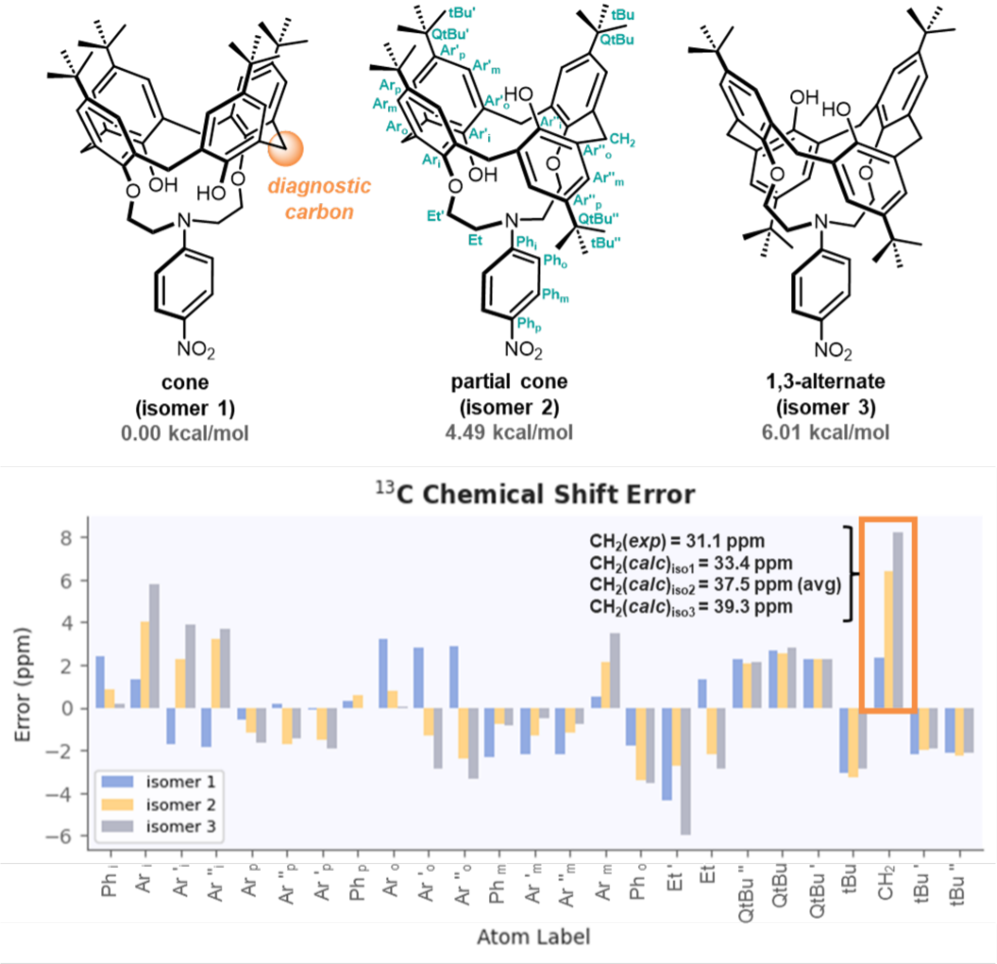

Figure 8: Computational analysis of bridged calix[4]arene derivative # conformations. (Top) Structures of the three main conformations of # with their respective common names, isomer numbers, and energies calculated at the M06-2X/6-31G(d,p) level of theory. (Bottom) Plot of error in ppm (y-axis) at each carbon (x-axis; labels correspond to those on isomer 2 above) from Boltzmann-weighted ^{13}C NMR chemical shift calculations. The orange box highlights the diagnostic methylene carbon (as indicated on the above structure of isomer 1) at which chemical shifts are distinct for each conformation.

NMR spectra. We also studied the capability of 2D NMR techniques including NOESY and ROESY to provide conformational geometry. These analyses were complicated by the fact that the calix[4]arene crown was found to take on an asymmetrical oval shape, a consequence of the effect of the bridge on the symmetry structure of the molecule. This resulted in otherwise-equivalent NMR protons appearing at several different distances in our calculated structures. While NOESY provided only tentative hints toward the cone geometry through apparent proximity of protons on the relevant phenol groups, the ROESY spectrum was conclusive in identifying a CH_2 to the Ph_{bridge} distance of 2.42 ± 0.14 that was consistent only with the cone conformer. The methods we have demonstrated may find wider use in the analysis of complex calix[4]arene molecules and their 3D geometry and conformational structure

Acknowledgements

We acknowledge support from the US National Science Foundation under award number NSF CHE 2004111 and the Robert A Welch Foundation under award number Y-2031-20200401 (University of Texas Arlington) the US Department of Energy under awards DE-SC0019054 and DE-SC0019223.

References

(1) Gutsche, C. D. Calixarenes H/C. 1989.

(2) Zhang, D.; Crawford, J. D.; Bartsch, R. A. Di-ionizable p-tert-butylcalix [4] arene-1, 2-monothiacrown-3 ligands in the cone conformation: synthesis and metal ion extraction. *Tetrahedron* **2008**, *64*, 9843–9849.

(3) Zhou, H.; Liu, D.; Gega, J.; Surowiec, K.; Purkiss, D. W.; Bartsch, R. A. Effect of para-substituents on alkaline earth metal ion extraction by proton di-ionizable calix [4]

arene-crown-6 ligands in cone, partial-cone and 1, 3-alternate conformations. *Organic & Biomolecular Chemistry* **2007**, *5*, 324–332.

(4) Li, G.-K.; Xu, Z.-X.; Chen, C.-F.; Huang, Z.-T. A highly efficient and selective turn-on fluorescent sensor for Cu 2+ ion based on calix [4] arene bearing four iminoquinoline subunits on the upper rim. *Chemical communications* **2008**, 1774–1776.

(5) Wieser, C.; Matt, D.; Fischer, J.; Harriman, A. Capping calixarenes with metallodiphosphine fragments: towards intracavity reactions. *Journal of the Chemical Society, Dalton Transactions* **1997**, 2391–2402.

(6) Sharma, S. K.; Gutsche, C. D. Upper Rim Substitution of Calix [4] arenes via Their Upper Rim A, C Dinitro Compounds (1). *The Journal of organic chemistry* **1999**, *64*, 998–1003.

(7) Van Dienst, E.; Bakker, W. I.; Engbersen, J. F.; Verboom, W.; Reinhoudt, D. N. Calixarenes, chemical chameleons. *Pure and applied chemistry* **1993**, *65*, 387–392.

(8) Becke, A. D. Densityfunctional thermochemistry. III. the role of exact exchange. 98 (7): 5648–5652. *The Journal of Chemical Physics. doi: https://doi. org/10.1063/1.464913* **1993**,

(9) Lee, C.; Yang, W.; Parr, R. G. Development of the Colle-Salvetti correlation-energy formula into a functional of the electron density. *Physical review B* **1988**, *37*, 785.

(10) Ditchfield, R.; Hehre, W. J.; Pople, J. A. Self-consistent molecular-orbital methods. IX. An extended Gaussian-type basis for molecular-orbital studies of organic molecules. *The Journal of Chemical Physics* **1971**, *54*, 724–728.

(11) Hehre, W. J.; Ditchfield, R.; Pople, J. A. Self—consistent molecular orbital methods. XII. Further extensions of Gaussian—type basis sets for use in molecular orbital studies of organic molecules. *The Journal of Chemical Physics* **1972**, *56*, 2257–2261.

(12) Eddaif, L.; Shaban, A.; Telegdi, J. Sensitive detection of heavy metals ions based on the calixarene derivatives-modified piezoelectric resonators: A review. *International Journal of Environmental Analytical Chemistry* **2019**, *99*, 824–853.

(13) Jaime, C.; De Mendoza, J.; Prados, P.; Nieto, P. M.; Sanchez, C. Carbon-13 NMR chemical shifts. A single rule to determine the conformation of calix [4] arenes. *The Journal of Organic Chemistry* **1991**, *56*, 3372–3376.

(14) Xie, R.; Li, Y.; Tang, P.; Yuan, Q. Rational design, synthesis and preliminary antitumor activity evaluation of a chlorambucil derivative with potent DNA/HDAC dual-targeting inhibitory activity. *Bioorganic & medicinal chemistry letters* **2017**, *27*, 4415–4420.

(15) Li, G.; Guan, Y.; Ye, F.; Liu, S. H.; Yin, J. Cyanine-based fluorescent indicator for mercury ion and bioimaging application in living cells. *Spectrochimica Acta Part A: Molecular and Biomolecular Spectroscopy* **2020**, *239*, 118465.

(16) Gutsche, C. D.; Iqbal, M. p-tert-Butylcalix [4] arene. *Organic Syntheses* **2003**, *68*, 234–234.

(17) Pracht, P.; Bohle, F.; Grimme, S. Automated exploration of the low-energy chemical space with fast quantum chemical methods. *Physical Chemistry Chemical Physics* **2020**, *22*, 7169–7192.

(18) Smith, S. G.; Goodman, J. M. Assigning the stereochemistry of pairs of diastereoisomers using GIAO NMR shift calculation. *The Journal of Organic Chemistry* **2009**, *74*, 4597–4607.

(19) Kevin, E.; Jonathan, M.; others The optimal DFT approach in DP4 NMR structure analysis–pushing the limits of relative configuration elucidation. *Organic & Biomolecular Chemistry* **2019**, *17*, 5886–5890.

(20) Grimblat, N.; Zanardi, M. M.; Sarotti, A. M. Beyond DP4: An improved probability for the stereochemical assignment of isomeric compounds using quantum chemical calculations of NMR shifts. *The Journal of organic chemistry* **2015**, *80*, 12526–12534.

(21) Smith, S. G.; Goodman, J. M. Assigning stereochemistry to single diastereoisomers by GIAO NMR calculation: The DP4 probability. *Journal of the American Chemical Society* **2010**, *132*, 12946–12959.

(22) Cho, J.; Lee, S.; Hwang, S.; Kim, S. H.; Kim, J. S.; Kim, S. Calix [2] triazole [2] arenes; A class of hybrid heterocalixarenes. *European Journal of Organic Chemistry* **2013**, *2013*, 4614–4623.

(23) Burilov, V. A.; Fatikhova, G. A.; Dokuchaeva, M. N.; Nugmanov, R. I.; Mironova, D. A.; Dorovatovskii, P. V.; Khrustalev, V. N.; Solovieva, S. E.; Antipin, I. S. Synthesis of new p-tert-butylcalix [4] arene-based polyammonium triazolyl amphiphiles and their binding with nucleoside phosphates. *Beilstein journal of organic chemistry* **2018**, *14*, 1980–1993.

(24) Brouwer, E. B.; Udachin, K. A.; Enright, G. D.; Ripmeester, J. A.; Ooms, K. J.; Halchuk, P. A. Self-inclusion and paraffin intercalation of the p-tert-butylcalix [4] arene host: a neutral organic clay mimicIssued as NRCC No. 43878. *Chemical Communications* **2001**, 565–566.

(25) Neuhaus, D. Nuclear overhauser effect. *eMagRes* **2007**,

(26) Wu, J.; Lorenzo, P.; Zhong, S.; Ali, M.; Butts, C. P.; Myers, E. L.; Aggarwal, V. K. Synergy of synthesis, computation and NMR reveals correct baulamycin structures. *Nature* **2017**, *547*, 436–440.

(27) Schatz, J. Recent application of ab initio calculations on calixarenes and calixarene complexes. A review. *Collection of Czechoslovak chemical communications* **2004**, *69*, 1169–1194.